One-pot green synthesis of reduced graphene oxide decorated with β-Ni(OH)2-nanoflakes as an efficient electrochemical platform for the determination of antipsychotic drug sulpiride

Mona Mohamed, Shimaa Atty, Aml Asran, Rabah Boukherroub

One-pot green synthesis of reduced graphene oxide decorated with β-Ni(OH)₂-nanoflakes as an efficient electrochemical platform for the determination of antipsychotic drug Sulpiride

Mona A. Mohamed[1,2][*], Shimaa A. Atty[1], Aml M. Asran[3,4], Rabah Boukherroub[2]

[1]*Pharmaceutical Chemistry Department, National Organization for Drug Control and Research (NODCAR), Giza, Egypt*
[2]*Univ. Lille, CNRS, Centrale Lille, ISEN, Univ. Valenciennes, UMR 8520-IEMN, F-59000, Lille, France*
[3]*Preparatory Year Deanship, El-Jouf University, El-Jouf, Saudi Arabia*
[4]*Faculty of Engineering, Modern Academy for Technology and Engineering, Cairo, Egypt*

*To whom correspondence should be addressed:

Mona A Mohamed: monagamall77@gmail.com

1

Abstract

A promising electrochemical platform was fabricated for the quantification of a typical antipsychotic drug, Sulpiride (SUL), in different human fluids. The proposed electrochemical sensor was fabricated using β-Ni(OH)$_2$, reduced graphene oxide (Gr) and ionic liquid (IL). The designed sensor (Ni(OH)$_2$.Gr-IL/CPE) integrates the features of nanostructured β-Ni(OH)$_2$, Gr, and IL to achieve a high response and best sensitivity. Square wave voltammetry (SWV) was used for the detection of SUL in different complex matrices, while different techniques were utilized to characterize the proposed sensor features. Applying the optimal conditions, the developed platform exhibited a wide linear range 1.0×10^{-9} to 2.0×10^{-4} mol L^{-1} with a calculated limit of detection 2.50×10^{-10} mol L^{-1}. Furthermore, the designed sensor displayed good stability, selectivity and reproducibility, allowing the quantitative analysis of SUL in pharmaceutical preparation, human plasma and urine. The established electrochemical sensor is a potential prototype that can be applied in quality control work in the pharmaceutical industry.

Keywords: *β-Ni(OH)$_2$ nanoflakes; Graphene; Modified electrochemical sensors; Antipsychotic drugs; Real samples analysis.*

1. Introduction

Schizophrenia is a serious mental illness accompanied by 'positive symptoms' like delusions and hallucinations [1]. Schizophrenia represents one of the most disabling psychiatric disorders: it is the 8th leading cause of disability in the age group of 15–44 years [2], with a worldwide prevalence around 1% [3]. Patients with schizophrenia are mainly treated with antipsychotic medications. Modern advanced antipsychotic drugs are considered more costly and thought to have less side effects than the older ones (first generation or typical). As the case in the developing countries, the medication cost is a major issue in the prescribing, which in turn makes the first generation drugs an easy alternative and more common to be used [1]. Sulpiride (SUL) is a type of benzamide first generation antipsychotic medication. SUL also may be more efficient than other older drugs like haloperidol and chlorpromazine for the remediation of negative symptoms and social withdrawal of schizophrenia [1]. Lately, schizophrenia experienced an important growth in many countries like China, consequently, sulpiride is widely used in medical applications and administrated in a large dose for typical acute treatment [4, 5]. Chemically, SUL is 5-(aminosulfonyl)-N-[(1-ethyl-2-pyrrolidi-nyl) methyl]-2-methoxy-benzamide. It is commonly approved in psychiatric disorders which has the action of dopamine D_2 antagonist with an elevating mood and antipsychotic effect [6].

Antiepileptics are prescribed for the treatment of many psychiatric disorders and are commonly co-administered with other psychotropic drugs [6]. Sulpiride is among drugs used for augmentation of treatment with clozapine (CLO) and co-prescription was common [7], **Scheme 1**. So, due to the above mentioned importance of this drug, there is a great challenge in the determination and monitoring its concentration to avoid overdose that will be accompanied with dangerous side effects, especially in case of patients with mental diseases.
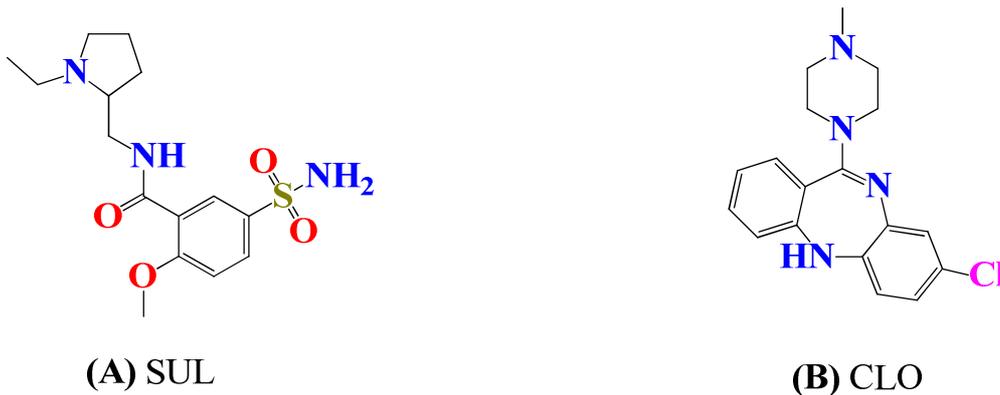
Scheme 1: Chemical structure of sulpiride (SUL) and clozapine (CLO).

To this end, different analytical techniques have been investigated for the determination of SUL, like electrophoresis [8, 9], spectrophotometry [10], adsorptive stirring voltammetry [11], flow injection chemiluminometry [12], fluorimetry [13], thin layer chromatography (TLC) [14], and high performance liquid chromatography [14-19].

Nowadays, much attention has been directed towards the use of nanomaterials as incorporated constituents in biosensing technology for the determination of many pharmaceutical drugs. Electrochemical sensing protocols have shown appropriate results for toxicity detection, environmental control, and food safety [20-26]. Since its discovery in 2004 [27], graphene and its derivatives have been widely investigated for their potential applications in various fields ranging from electronics, sensing to biomedicine [28-30]. Graphene exhibits interesting features such as outstanding conductivity, extraordinary electrocatalytic activity, high developed surface area, excellent charge transfer rate, and high mechanical strength [31, 32]. Reduced graphene oxide (Gr) is commonly produced through graphene oxide (GO) precursor reduction. Nevertheless, graphene is a hydrophobic material and tends to agglomerate due to van der Waals and strong π-π stacking interactions [33]. Through the integration of nanomaterials on the Gr surface, the problem of aggregation could be reduced or banned [34].

In this context, several materials including conducting polymers, transition metal oxides, and metal hydroxides, were examined vastly for a wide range of applications such as supercapacitors [35, 36] and electrochemical sensors [26]. Hitherto, $Ni(OH)_2$ has been considered as an interesting choice in many electrochemical applications due to its high surface area, and good redox performance. Also, $Ni(OH)_2$ is environmentally friendly and low-cost [37].

It is well known that nickel hydroxide has two polymorphs: α- and β-Ni(OH)$_2$ [38]. The β-phase displays greater stability in comparison to the α-Ni(OH)$_2$ [39]. Moreover, Gr based nanocomposites have been designed with the aim to enhance the electrochemical performance of modified sensors [40]. Furthermore, literature survey revealed that Ni and Ni oxide based sensors (Ni, Ni(OH)$_2$, NiO) exhibit superior sensing properties owing to the existence of Ni(OH)$_2$/NiOOH redox couple on the electrode surface in a basic medium [41, 42].

Ionic liquids recently have received excessive consideration in several fields especially in electrochemistry due to their exceptional characteristics including high viscosity, non-volatility, high ionic conductivity, oxidative and thermal stability, large solvation power and non-flammability [43, 44].

According to the previous published literature, there are no reports on the electrochemical determination of SUL using Ni(OH)$_2$.Gr-IL/CPE. Accordingly, the present work takes advantage of the unique properties of Ni(OH)$_2$, Gr, and ionic liquid for the construction of precise and selective platform for the determination of SUL in serum, urine and pharmaceutical products. The fabricated platform consists of 3D Ni(OH)$_2$ supported on IL modified Gr deposited on a carbon paste sensor. The morphology and chemical composition of the fabricated electrochemical platform was assessed using various techniques. The resulting sensor was utilized for the sensitive and selective determination of SUL alone and in the presence of clozapine (CLO).

2. Experimental

2.1. Apparatus

A Bio-logic SP 150 electrochemical workstation was used for analyzing the electrochemical properties of the samples. A one compartment cell with a three electrode set-up was connected to the electrochemical workstation through a C3-stand from BAS (USA). A platinum wire from BAS (USA) was employed as the auxiliary electrode. All the cell potentials were measured with respect to an Ag/AgCl (3.0 mol L^{-1} NaCl) reference electrode from BAS (USA). A Cyberscan 500 digital (EUTECH Instruments, USA) pH-meter with a glass combination electrode served to carry out pH measurements. All the electrochemical experiments were performed at an ambient temperature of 25°C. Impedance spectra were recorded over a frequency range from 100 mHz to 100 kHz.

5

Scanning electron microscopy (SEM) and energy-dispersive X-ray (EDX) were performed using a JSM-6700F scanning electron microscope (Japan Electro Company). FT-IR spectra were recorded on an IR-Affinity-1 Fourier Transform Infrared Spectrophotometer (Shimadzu, Japan). The crystalline phases were detected and identified using an X-ray diffractometer (XRD) on an X'Pert PRO MRD with a copper source at a scan rate 2θ of $1^{o}s^{-1}$. Sigma Plot 10.0 was used for all statistical data.

2.2. Reagents and solutions

All the chemicals were of analytical grade and used without further purification. A sulpiride (SUL) stock solution (1.0×10^{-3} mol L^{-1}) was prepared in ultra-pure water and stored in the dark at 4 ^{o}C. Britton–Robinson (B–R; 0.04 mol L^{-1}) supporting electrolyte buffer solutions of pH range (2.0–9.0) (CH_3COOH, H_3BO_3 and H_3PO_4) were used and adjusted using 2.0×10^{-3} mol L^{-1} NaOH. Dogmatil Fort® tablet 200 mg/Tablet was supplied from Sanofi-Aventis Egypt. Fresh human plasma was obtained from the blood bank (VACSERA, Cairo, Egypt).

2.3. Synthesis of Ni(OH)₂.Gr nanocomposites

Graphene oxide (GO) was synthesized from graphite powder using the Hummers' method [45]. Ni(OH)₂.Gr nanocomposites were prepared hydrothermally as follows. In short, 0.092 g of GO were dispersed in 30 mL distilled water for 1 h with the aid of ultrasonication to obtain a homogeneous solution. Next, 2.90 g $Ni(NO_3)_2 \cdot 6H_2O$ were dissolved in 20 mL distilled water and added to the GO solution. The temperature of the solution was raised to 60 ^{o}C and its pH was adjusted to 10.0 using 4.0 M NaOH. After stirring for 2 h, the resulting suspension was transferred into 80 mL Teflon-lined stainless steel auto-clave. The volume was completed to 70 mL with ethanol. The autoclave was sealed and placed in an oven at 160 °C for 14 h for hydrothermal treatment. The autoclave was then allowed to cool at room temperature. The product was washed with deionized water several times and dried at 50 °C for 24 h.

2.4. Preparation of different electrodes used in this study

Carbon Paste Electrodes (CPE) were prepared using the procedure reported in our previous works [20, 21, 46]. Accordingly, a few drops of paraffin oil were mixed with graphite powder (0.5 g) using a pestle and mortar. The resulting paste was packed into the cavity of the electrode body and smoothed on paper. For the preparation of Ni(OH)₂.Gr-IL modified sensor (Ni(OH)₂.Gr-IL/CPE), graphite powder (5.0 wt.%) was mixed with Ni(OH)₂.Gr and 10 µL ionic

liquid (IL). Ni(OH)$_2$.Gr/CPE and IL/CPE were prepared using the same procedure for comparison.

The electroactive area of the electrode was obtained by the cyclic voltammetric method using 5.0 mM K$_3$Fe(CN)$_6$ in 0.1 M KCl at different scan rates, using the Randles-Ševčík [47]. The calculated areas were 0.055, 0.077, 0.111, 0.122, 0.121 and 0.150 cm^2 for CPE, GO/CPE, Ni(OH)$_2$.Gr/CPE, IL/CPE, and Ni(OH)$_2$.Gr-IL/CPE sensors, respectively.

2.5. Recommended experimental procedure

A stock solution of SUL (1.0×10^{-3} mol L^{-1}) was prepared in double distilled water. The essential amount of any of this stock solution was transferred to a 5.0 mL standard volumetric flask, in which the solution volume was completed to the mark using 4.0×10^{-2} mol L^{-1} Britton–Robinson buffer (B-R) solution (pH 7.0).

Prior to voltammetric measurements, the modified electrode (Ni(OH)$_2$.Gr-IL/CPE) was cycled several times between 0 to +1200 mV at a scan rate of 100 mV s^{-1} in B-R buffer of pH 7.0 till a reproducible behavior was obtained. Then, Ni(OH)$_2$.Gr-IL/CPE electrode was placed into a different cell containing a proper amount of SUL in B-R buffer of pH 7.0. Cyclic voltammograms or SWV were recorded using the same parameters.

For SWV measurements, aliquots with SUL concentrations from 1.0×10^{-9} to 2.0×10^{-4} mol L^{-1} were placed in a series of 5.0 mL volumetric flasks using a micropipette. The volume was then made to the flask mark by adding B-R buffer (pH 7.0). By transferring 5 mL of the solution to the electrolytic cell, SWV was ready to record. A scan rate of 100 mVs^{-1} was used to record the current response of SWV measurements at the Ni(OH)$_2$.Gr-IL/CPE working electrode. Also, the pulse period during chronoamperometry was 30 s *vs*. Ag/AgCl, while the impedance measurements were performed over a frequency range of 100 mHz − 100 kHz.

2.6. Preparation of spiked plasma and urine samples

Immediately prior to electrochemical measurements, plasma/urine samples were drawn from a healthy individual, in which 10 µL of the sample was injected into a 5-mL volumetric flask spiked with 2.0×10^{-4} mol L^{-1} of SUL standard solution of different volumes, containing B-R buffer (pH 7.0). Then, the solution was directly transferred to the voltammetric cell for analysis. The experimental measurements were all carried out in accordance with the institutional

guidelines and conventional laws, after having the approval of the institutional ethics committees.

3. Results and discussion

3.1. Characterization of the prepared nanocomposite

The structure of the synthesized materials was investigated by X-ray diffraction pattern (XRD). The XRD pattern of graphite flakes displays a sharp strong peak at 26.26°, indicating a highly ordered structure [48]. After extensive oxidation and graphite exfoliation to yield graphene oxide (GO), the XRD data displayed a characteristic (002) GO peak at $2\theta = 10°$, **Figure 1**. Obviously, the XRD pattern of Ni(OH)$_2$.Gr comprised seven diffraction peaks at 19.2°, 33.1°, 38.7°, 59.2°, 62.8°, 70.5 and 72.6° that could be indexed as: (0 0 1), (1 0 0), (1 0 1), (1 1 0), (1 1 1), (1 0 3) and (2 0 1) of β-phase Ni(OH)$_2$ [49], in good agreement of the transformation of elemental nickel to hexagonal β-phase Ni(OH)$_2$ after the hydrothermal treatment [50]. The diffraction peak generated from the reduction of graphene oxide (Gr) disappeared in the XRD chart of Ni(OH)$_2$.Gr sample, most likely due to a higher disordered stacking in the as-prepared composites and fairly uniform dispersion of resulted graphene sheets [51].
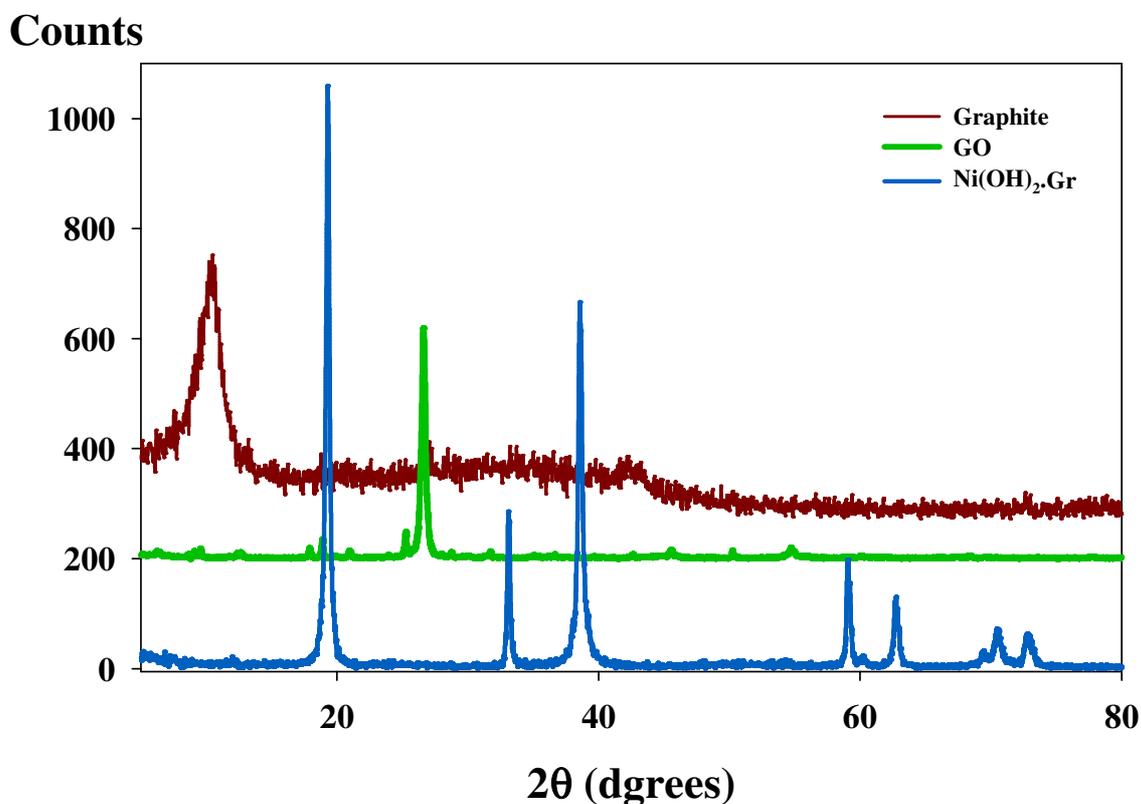
Figure 1. XRD patterns of graphite, GO, and Ni(OH)$_2$.Gr.

To confirm the XRD outputs, the chemical composition of Ni(OH)$_2$.Gr was studied using FTIR in the 400–4000 cm^{-1} range and the outcomes were presented in **Figure 2A**. A band located at around 3639 cm^{-1} is attributed to the hydroxyl groups in the brucite-like form [39, 52]. The broad band at 3435 cm^{-1} is assigned to the inter-lamellar H$_2$O and HO-bond vibrations of the hydrogen-bonded hydroxyl groups and interpolated H$_2$O molecules present in the inter-lamellar area of Ni(OH)$_2$ [39, 53]. The weak band at around 1585 cm^{-1} is due to the bending mode of the interlayer H$_2$O molecules and the carbon ring vibration in the Gr sheets [27]. Moreover, the absorption band located at 1200 cm^{-1} is possibly due to the existence of carbonate ions derived from the adsorption of atmospheric CO$_2$ [35]. Additionally, the band at 1375 cm^{-1} is assigned to the nitrate anion interlayer [35, 54], while the two bands at around 424 and 541 cm^{-1} are attributed to the vibrations of Ni-OH and OH groups [39, 55], respectively.
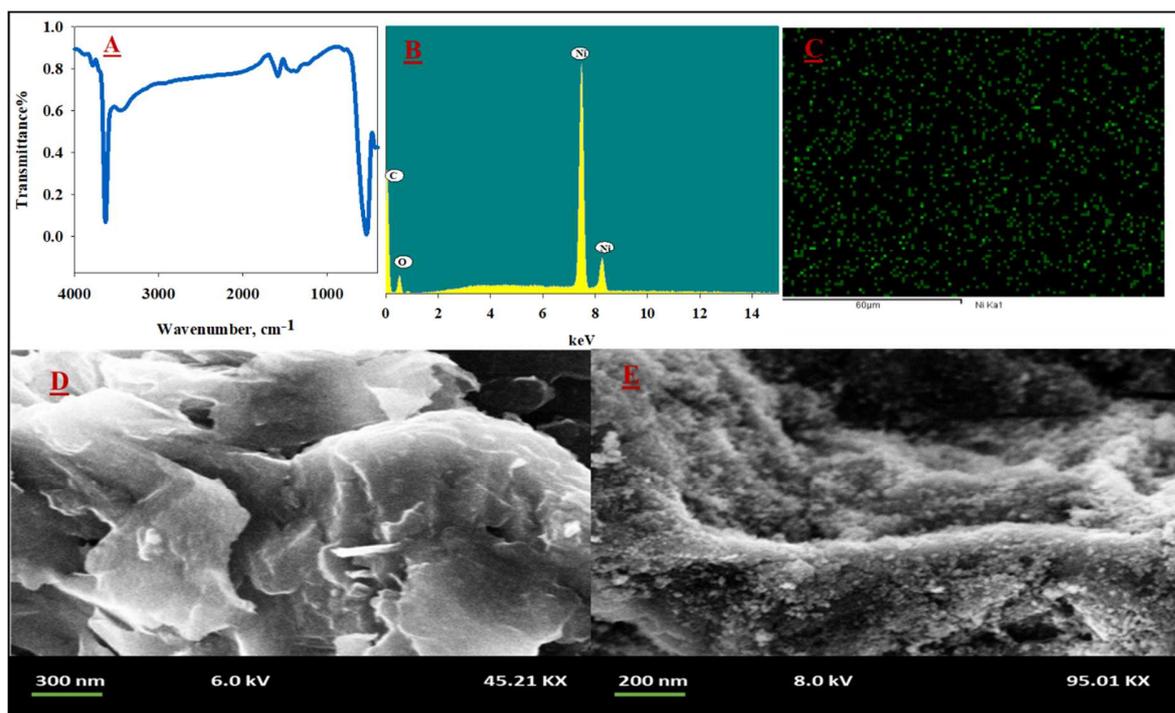

Figure 2. (A) FTIR spectrum, (B) EDX spectrum, (C) EDX surface imaging of Ni(OH)$_2$.Gr, (D) SEM of GO, and (E) SEM of Ni(OH)$_2$.Gr.

Surface morphology and EDX-mapping of Ni(OH)$_2$.Gr revealed that carbon, oxygen, nickel are the main element (**Fig. 2B** and **2C**) with uniform distribution of Ni(OH)$_2$ on the Gr

nanosheets. Apparent signature peaks of C, O and Ni were observed, which indicates the successful integration of Ni(OH)$_2$ with Gr.

The microstructures of the as-prepared samples were analyzed by SEM. Figure 2D shows the flake-like shape and layer–layer structure of GO edges. While the difference in structure is clear in Figure 2E, the as-grown Ni(OH)$_2$ nanoplates not only exist on the surface but also are wrapped in the inner of the hole walls which contain of thin layers of stacked graphene sheets. Scheme 2 represents the preparation of Ni(OH)$_2$.Gr through hydrothermal method.
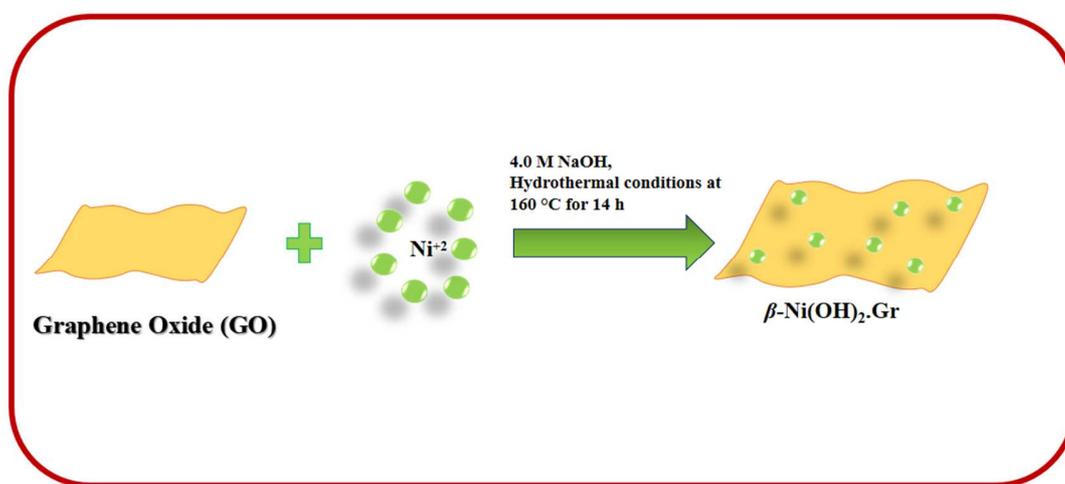
Scheme 2. Schematic representation for the preparation of Ni(OH)$_2$.Gr nanocomposite.

The prepared material studied exhibited an excellent catalytic activity, which makes it an ideal choice for the modification of electrochemical sensors. Additional study revealed that the performance enhancement can be associated with relatively well ordered assembly of graphene and β-Ni(OH)$_2$ particles. Moreover, this material was prepared via a low-cost precursors and moderate conditions, which can be easily adaptable for large-scale synthesis. Importantly, this simple synthesis strategy can be easily extended to the preparation of other graphene-based 3D catalysts for a broad range of technological applications including metal–air batteries, photocatalysis and heterocatalysis.

3.2. Electrochemical behavior of SUL at different sensors

Square wave voltammetry (SWV) was applied to assess the performance of the different electrochemical platforms for SUL in B-R buffer (pH 7.0); all electrochemical measurements were recorded at a scan rate of 100 mV s^{-1} over the potential range 0.2 to -1.15 V using $2.0 \times 10^{-}$

[4] mol L^{-1} of SUL, **Figure 3A**. In case of bare CPE, the anodic peak current, which represents the oxidation of SUL, was 20.19 µA at +0.77 V. Note that the value of the voltammetric signal of the electrochemical platform increases upon GO nanosheets integration where the peak of oxidation appears at +0.76 V with a value of 25.70 µA. Upon introducing Ni(OH)$_2$.Gr nanocomposite, the current increased to 30.23 µA at +0.75 V. Next, the voltammetric signal is further enhanced through the incorporation of IL, as evidenced in **Fig. 3A**, as the Ip increased to a value of 30.19 µA at +0.74 V. More interestingly, the oxidation peak current further increased to 50.53 µA at +0.72 V using Ni(OH)$_2$.Gr-IL/CPE. Thus, Ni(OH)$_2$.Gr and IL potentially act as promoters/mediators to enhance the electron transfer rate as a result of their high surface area, catalytic capabilities, and the highest sensitivity among these modified electrodes as the higher signal refers to higher sensitivity for SUL.
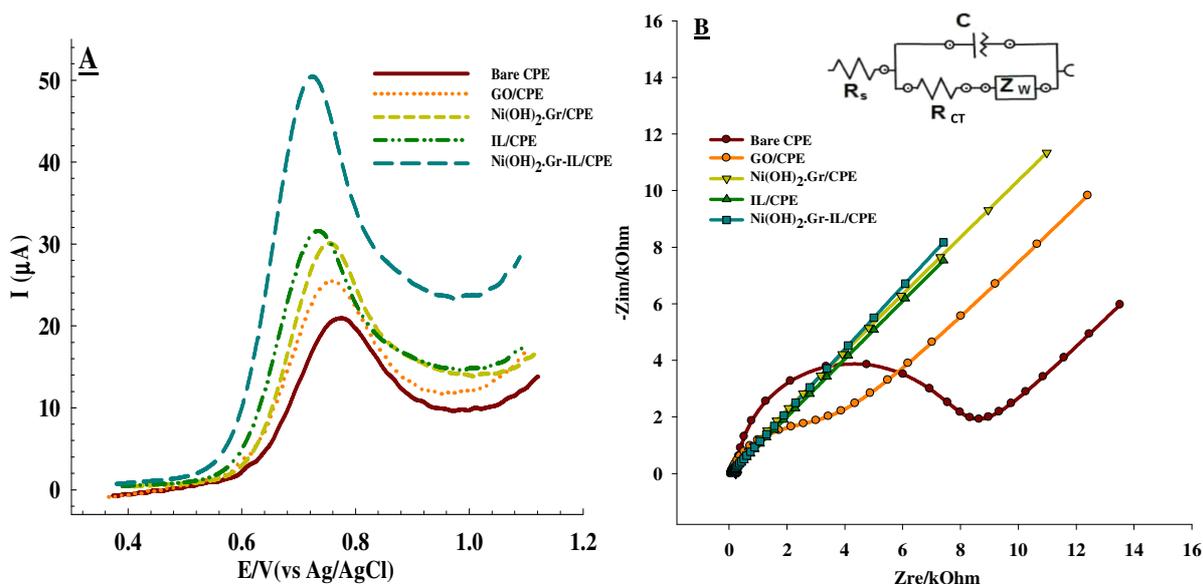

Figure 3. (A) Square wave voltammograms of 2.0×10^{-4} mol L^{-1} SUL in B-R buffer (pH 7.0) recorded at a scan rate of 100 mV s^{-1} on bare CPE, GO/CPE, Ni(OH)$_2$.Gr/CPE, IL/CPE, and Ni(OH)$_2$.Gr-IL/CPE, (B) the corresponding impedance plots at a scan rate of 100 mV s^{-1} in 5.0 mol L^{-1} K$_3$Fe(CN)$_6$ (1:1) solution in 0.1 mol L^{-1} KCl.

Electrochemical impedance spectroscopy (EIS) is considered as a valuable tool for accurate calculation of different parameters including mass transport and charge transfer coefficient. **Figure 3B** displays the EIS signals of the different studied sensors in 5.0 mM

$K_3Fe(CN)_6$ (1:1) solution in 0.1 M KCl. By fitting the EIS data, an equivalent circuit was chosen as the resistance was modeled for the charge transfer R_{CT}, while the Warburg-type impedance (W) was chosen for the diffusion process. Both elements were in parallel with the interfacial capacitance (C).

As depicted in **Figure 3B**, the bare CPE revealed a very large semicircle domain, attributed to a very high electron transfer resistance of the redox probe. Upon modification of CPE with GO, $Ni(OH)_2$**.**Gr or IL, the Nyquist plots showed a small semicircle domain, suggesting enhanced conductivity. When the CPE electrode was coated with $Ni(OH)_2$**.**Gr-IL, the R_{CT} decreased, indicating an increased ability of the redox probe to electron transfer. R_{CT} was determined to be 6294.0 Ω for CPE, whereas this value decreased to 2500.0, 420.0, 400.0 and 186.0 Ω for GO/CPE, $Ni(OH)_2$**.**Gr/CPE, IL/CPE, $Ni(OH)_2$**.**Gr-IL/CPE, respectively, demonstrating that the $Ni(OH)_2$**.**Gr-IL offers the greatest conduction of electrons as a result of the interactive properties of the electrode compositions.

## 3.2. Influence of $Ni(OH)_2$**.**Gr and IL content

The influence of $Ni(OH)_2$**.**Gr and IL content utilized in the construction of the $Ni(OH)_2$**.**Gr-IL/CPE on the sensor performance was assessed. The peak signal of SUL oxidation at $Ni(OH)_2$**.**Gr-IL/CPE was investigated as a function of the amount of $Ni(OH)_2$**.**Gr (2.0-30.0%). It was found that the highest current was detected when the CPE was composed of a quantity equivalent to 5% of $Ni(OH)_2$**.**Gr nanocomposite, **Figure S1**. While, 10 µL of IL was sufficient to achieve the highest response, as further addition results in a distortion in peak sharpness.

3.3. Effect of solution pH

The selection of an appropriate electrolyte is essential in electroanalytical applications, since it affects the analyte signal in terms of peak potential and height. The influence of solution pH (2.0-9.0) of the B-R buffer on the electrochemical oxidation of 2.0×10^{-4} mol L^{-1} was studied using square wave voltammetry. **Figure 4** reveals that the Ep shifts to more negative potentials upon increasing the pH from 2.0 to 9.0. **Figure 4** displays the relationship of the Ip and Ep with buffer pH. The peak current increased with increasing the buffer pH. In neutral pH buffer solution, more protons can be provided, which are useful for the redox reaction of SUL. Consequently, pH 7.0 B-R buffer was chosen as the appropriate pH for further investigations.

Examination of the voltammetric response in terms of peak potential (Ep) reveals a straight relationship with the pH, which can be fitted as: E_p (V) = 1.068 V - 50.1 mVpH^{-1}, (R^2 = 0.9996). The suggested reaction mechanism of SUL is depicted in **Scheme 3**.
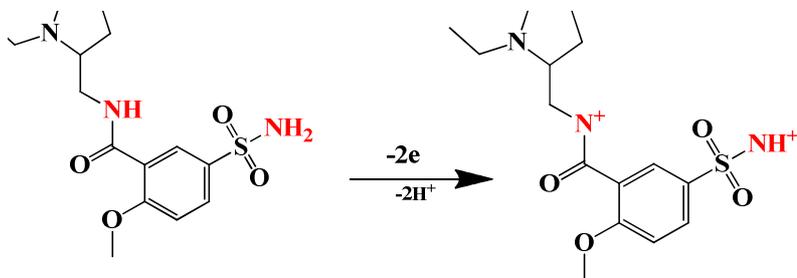
Scheme 3. The suggested reaction mechanism of SUL.
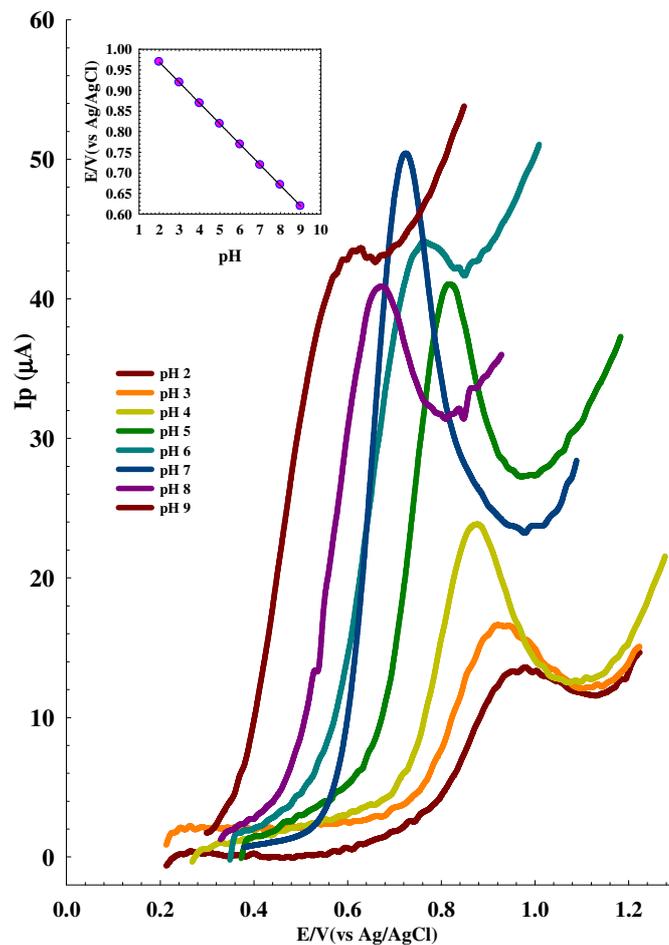
Figure 4. Square wave voltammetric responses of 2.0×10^{-4} mol L^{-1} SUL at different pH values (2.0-9.0) using Ni(OH)$_2$**.**Gr-IL/CPE sensing platforms at a scan rate of 0.1 V s^{-1}. The inset displays the relation of I$_P$ *versus* pH.

3.4. Scan rate optimization

Next, the mechanism of the electrochemical reaction can be assessed through the investigation of the influence of scan rate (*v*) of the oxidation peak signal by CV at Ni(OH)$_2$**.**Gr-IL/CPE in 2.0×10^{-4} mol L^{-1} SUL in B-R buffer (pH 7.0). The result is illustrated in **Figure S2**. Upon increasing the potential scan rate in the 10-200 mV s^{-1} range, the current value increased and the peak potential shifted to more positive values with no noticeable reverse reduction peak, suggesting that the oxidation of SUL is an irreversible process.

14

By plotting the peak current (I_{pa}) against the square root of the scan rate ($v^{1/2}$), a linear straight line was obtained (**Fig. S2**, inset A), indicating that the reaction is controlled by diffusion, according to:

$$I_p \, (\mu A) = 6.8611\sqrt{v} - 5.31; \; R^2 = 0.9995.$$

Direct relation was acquired between log Ip and log v in the 10 - 200 mVs^{-1} range as the following:

$$\log I(\mu A) = 0.6530 + 0.5756 \log v; \; R^2 = 0.9999.$$

The obtained slope value was 0.575 for Ni(OH)$_2$.Gr-IL/CPE sensor, which supports that the predominant process is diffusion controlled [56].

Furthermore, kinetic parameters were calculated for the electrochemical process on Ni(OH)$_2$.Gr-IL/CPE using the theory of Laviron for irreversible reactions. Since for a totally irreversible reaction, α (electron transfer coefficient) was assumed as 0.5, then n (the number of electrons transferred) was determined to be 2.4, suggesting that two electrons were involved in the oxidation of SUL. The value of k^o (the standard heterogeneous rate constant of the surface reaction) can be calculated from the intercept of Laviron equation and was determined to be 2.46 s^{-1}.

3.5. Chronoamperometry measurements (CA)

Chronoamperometry measurements were carried out for five different concentrations (2.40×10^{-7} mol L^{-1} to 1.11×10^{-4} mol L^{-1}) at an applied potential of +0.72 V to determine the apparent diffusion coefficient (D_{app}) of SUL in 0.04 mol L^{-1} at the selected pH, **Fig. S3.** Next, by rising the SUL content, a visible increase of Ip relative to the background could be distinguished. The increase of Ip is due to the influence of faradaic current from the oxidation of SUL taking place at +0.85 V. Cottrell's equation can explain the dependence of faradaic current chronoamperometrically measured versus time [57]. By plotting the Ip versus t$^{-1/2}$ plot (I vs. t$^{-1/2}$) for each individual SUL concentration and calculating the slopes which were then further plotted, inset (i) **Fig. S3**. The obtained slopes of each curve were then plotted vs. SUL

15

concentration. Finally, the D_{app} was calculated and found to be $1.88 \times 10^{-5}\, cm^2\, s^{-1}$ using Cottrell's equation [57].

3.6. Optimization of the developed analytical method

Through applying the guidelines of International Conference on Harmonization (ICH) [58], the developed electrochemical platform Ni(OH)$_2$.Gr-IL/CPE for the precise determination of SUL was validated. The superimposed SWV curves of variant SUL concentrations at pH 7.0 indicate that the I_{pa} is proportional to the SUL concentration in a linear dynamic range 1.0×10^{-9} to 2.0×10^{-4} mol L^{-1}, **Figure 4**. The resultant regression equation is: I_{pa} (µA) = 0.240 C (µmol L^{-1}) + 1.253 (R^2 = 0.9990). The SWV results are displayed in **Figure 6** along with the corresponding calibration plot (inset of **Figure 4**). The detection limit (LOD) and quantitation limit (LOQ) were determined to be 2.5×10^{-10} M and 8.33×10^{-10} M, respectively. The intermediate precisions and repeatability were investigated and found to be 1.23% and 1.17%, respectively. By comparing the suggested platform with the described electrochemical method in literature, Ni(OH)$_2$.Gr-IL/CPE exhibits the lowest limit of detection [11].
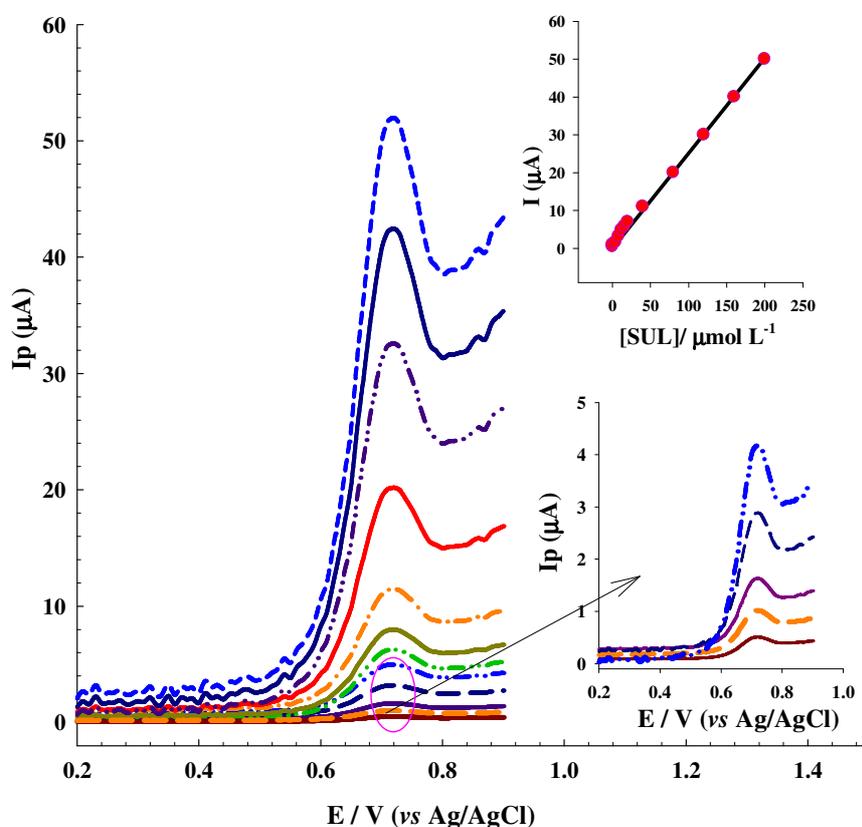
**Figure 4.** SWVs using Ni(OH)$_2$**.**Gr-IL/CPE sensing platform recorded in a B-R buffer (pH 7.0) corresponding to 1.0×10^{-9} to 2.0×10^{-4} M SUL at a scan rate: 100 mV s^{-1}, P$_H$= 0.25 V, P$_W$=0.50 V, S$_H$=0.02 V. The inset shows the plot of the peak current as a function of SUL concentration in the concentration range 1.0×10^{-9} to 2.0×10^{-4} mol L^{-1}.

To check the specificity of Ni(OH)$_2$**.**Gr-IL/CPE, its response was inspected for the analysis of SUL in the presence of co-administered medication Clozapine (CLO), **Figure 5**. CLO and SUL were determined simultaneously at the Ni(OH)$_2$**.**Gr-IL/CPE surface. **Figure 5** shows the SWVs curves of CLO and SUL. The obtained data displayed distinct sharp anodic peaks at +0.386 and +0.710 V corresponding to the oxidation of CLO and SUL, respectively, suggesting that the determination of these compounds is feasible even in presence of each other using the Ni(OH)$_2$**.**Gr-IL/CPE sensor.

Figure 5 displays the curve of the electroanalytical peak signal as a function of the SUL and CLO concentrations. The calibration plots were linearly related to CLO and SUL over the ranges of 4.0×10^{-6} - 2.0×10^{-4} mol L^{-1} and 4.0×10^{-6} -2.0×10^{-4} mol L^{-1}, respectively. The regression equations are: I$_p$(µA) = 0.243C (µmol L^{-1}) + 1.089, R^2= 0.9992 and I$_p$(µA) = 0.224C (µmol L^{-1}) + 0.988, R^2 = 0.9994 for CLO and SUL, respectively. Ni(OH)$_2$**.**Gr-IL/CPE oxidation sensitivity of SUL was found to be 0.240 µA/µM, which is close to the result calculated in the absence of CLO (0.224 µA/µM). Consequently, the determination of CLO and SUL at the Ni(OH)$_2$**.**Gr-IL/CPE occurs independently and therefore, their simultaneous detection can be achieved without inconsistency. Further discussion about interference, reproducibility and stability are presented in supplementary information.
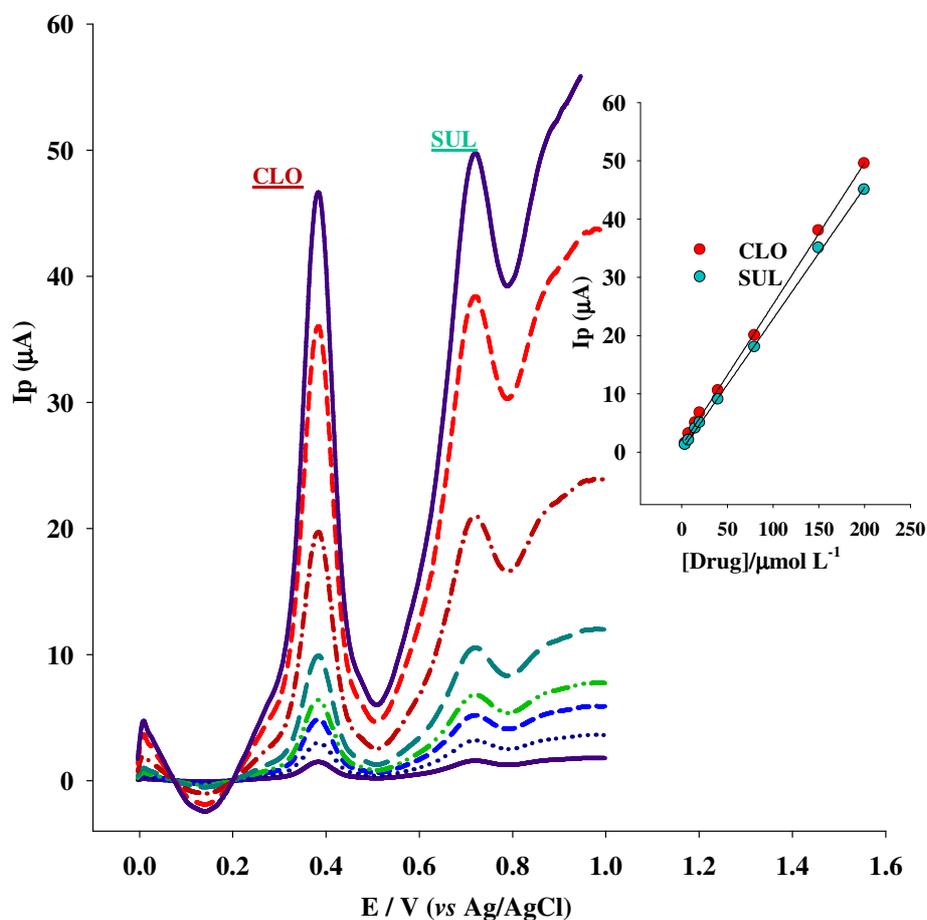
Figure 5. Square wave voltammograms using Ni(OH)$_2$**.**Gr-IL/CPE sensing platform in a BR buffer (pH 7.0) containing different concentrations of CLO and SUL corresponding to 4.0×10^{-6} - 2.0×10^{-4} for each at a scan rate= 100 mV s^{-1}, P$_H$= 0.25 V, P$_W$=0.50 V, S$_H$=0.02 V. Insets: the corresponding analytical curves. Insets: the plots of I$_p$ versus CLO and SUL concentrations.

3.6. Real samples analysis

To confirm the reliability of the suggested electrochemical platform for the sensitive determination of SUL, the concentration of the drug was detected in spiked blood plasma, urine and pharmaceutical sample Dogmatil Fort® at the Ni(OH)$_2$**.**Gr-IL/CPE sensor, **Table 1**. Inspection of the obtained recovery values proved high accuracy and sensitivity of the proposed sensor. Also, the platform has outstanding importance for the analysis of trace amounts of SUL

in pharmaceutical formulations and biological fluids. **Table 1.** Determination of SUL in pharmaceutical formulation Dogmatil Fort® and human plasma samples.

Sample	Amount added (M)	Amount found[a] (M)	Apparent recovery (%)
Plasma	5.00×10^{-6}	4.90×10^{-6}	98.00
	4.00×10^{-5}	3.93×10^{-5}	98.30
	3.00×10^{-4}	2.97×10^{-4}	99.01
Urine	5.00×10^{-6}	4.93×10^{-6}	98.70
	4.00×10^{-5}	3.94×10^{-5}	98.55
	3.00×10^{-4}	2.97×10^{-4}	99.12
Dogmatil Fort®	5.00×10^{-6}	5.05×10^{-6}	101.00
	4.00×10^{-5}	4.01×10^{-5}	100.32
	3.00×10^{-4}	2.98×10^{-4}	99.45

[a] Confidence interval with 95% probability calculated based on three replications.

3.7. Interference studies

Many substances which can possibly interfere with the electro-analytical determination of SUL were investigated using recommended conditions. Several main interfering species were selected, which are usually in the pharmaceutical preparations and other interfering ions, namely potassium sorbate, stearic acid, talc powder, magnesium stearate, povidone, microcrystalline cellulose, starch, cellulose, colloidal silicon dioxide, croscarmellose sodium, Cu^{2+}, Zn^{+2}, Mn^{+2}, Mg^{+2}, uric acid, and ascorbic acid, **Table S1**. By adding these interference species to a fixed SUL concentration of 1.0×10^{-5} M in a B-R buffer (pH 7.0), the current of SUL was recorded. From the selected materials, there was no interference obtained that could affect the electro-analytical sensing of SUL and the tolerance limit was less than ± 5 % for the selected interference substances, **Table S1**.

3.8. The reproducibility and stability of Ni(OH)$_2$.Gr-IL/CPE

The reproducibility of the proposed sensor was assessed by construction of eight electrodes in a similar way described in the experimental part. The relative standard deviation (RSD) for the Ip between electrodes is 2.55% for a SUL concentration of 1.0×10^{-5} M, which demonstrates an acceptable reproducibility for the fabrication procedure. The repeatability was examined by performing 6 times determination of a same standard solution (1.0×10^{-5} M of SUL). The RSD of the peak signals was determined to be 1.39%, indicating an excellent repeatability for Ni(OH)$_2$.Gr-IL/CPE. When the sensor was stored in air for three weeks, the peak current remained up to 98 % of its initial response. Therefore, the suggested sensor is appropriate for the routine analysis of SUL in biological fluids and pharmaceutical dosage form.

4. Conclusion

This work demonstrates the fabrication of a chemically modified carbon paste electrode (CPE) by the incorporation of β-Ni(OH)$_2$, ionic liquid (IL) and reduced graphene oxide (Gr). Through the synergy of the suggested modifiers, excellent electrocatalytic activity and voltammetric performances are achieved for sensing of sulpiride (SUL). The sensitivity for the determination of SUL by Ni(OH)$_2$.Gr-IL/CPE was more than two times higher than that of unmodified CPE. The electrochemical oxidation behavior of SUL on the new sensor was studied and established. The developed sensor exhibited high reproducibility, selectivity, and sensitivity with other advantages like time saving, simplicity and cost-effectiveness. Additionally, the proposed electrochemical sensor was utilized for the quantitative detection of SUL in tablets, urine and plasma.

References

[1] J. Wang, S. Sampson, Sulpiride versus placebo for schizophrenia, The Cochrane Library, (2014).

[2] W. Rössler, H.J. Salize, J. van Os, A. Riecher-Rössler, Size of burden of schizophrenia and psychotic disorders, European Neuropsychopharmacology, 15 (2005) 399-409.

[3] J. Perälä, J. Suvisaari, S.I. Saarni, K. Kuoppasalmi, E. Isometsä, S. Pirkola, T. Partonen, A. Tuulio-Henriksson, J. Hintikka, T. Kieseppä, Lifetime prevalence of psychotic and bipolar I disorders in a general population, Archives of general psychiatry, 64 (2007) 19-28.

[4] M.R. Phillips, Characteristics, experience, and treatment of schizophrenia in China, Dialogues in clinical neuroscience, 3 (2001) 109.

[5] J. Long, G. Huang, W. Liang, B. Liang, Q. Chen, J. Xie, J. Jiang, L. Su, The prevalence of schizophrenia in mainland China: evidence from epidemiological surveys, Acta Psychiatrica Scandinavica, 130 (2014) 244-256.

[6] L.S. Goodman, Goodman and Gilman's the pharmacological basis of therapeutics, McGraw-Hill New York, 1996.

[7] S. Porcelli, B. Balzarro, A. Serretti, Clozapine resistance: Augmentation strategies, European Neuropsychopharmacology, 22 (2012) 165-182.

[8] X. Xu, J.T. Stewart, Chiral analysis of selected dopamine receptor antagonists in serum using capillary electrophoresis with cyclodextrin additives, Journal of Pharmaceutical and Biomedical Analysis, 23 (2000) 735-743.

[9] J. Li, F. Zhao, H. Ju, Simultaneous electrochemiluminescence determination of sulpiride and tiapride by capillary electrophoresis with cyclodextrin additives, Journal of Chromatography B, 835 (2006) 84-89.

[10] M. Ghoneim, A.L. Saber, H. El-Desoky, Utility Spectrophotometric and Chromatographic Methods for Determination of Antidepressant Drug Sulpiride in Pharmaceutical Formulations and Plasma, Journal of Analytical & Bioanalytical Techniques, 5 (2014) 1.

[11] O.A.E.-M. Farghaly, Adsorptive stripping voltammetric determination of the antidepressant drug sulpiride, Journal of Pharmaceutical and Biomedical Analysis, 23 (2000) 783-791.

[12] F.A. Aly, N.A. Alarfaj, A.A. Alwarthan, Flow-injection chemiluminometric analysis of some benzamides by their sensitizing effect on the cerium-sulphite reaction, Talanta, 54 (2001) 715-725.

[13] A. Abdelal, N. El-Enany, F. Belal, Simultaneous determination of sulpiride and its alkaline degradation product by second derivative synchronous fluorescence spectroscopy, Talanta, 80 (2009) 880-888.

[14] I.A. Naguib, M. Abdelkawy, Development and validation of stability indicating HPLC and HPTLC methods for determination of sulpiride and mebeverine hydrochloride in combination, European Journal of Medicinal Chemistry, 45 (2010) 3719-3725.

[15] H. Kirchherr, W. Kühn-Velten, Quantitative determination of forty-eight antidepressants and antipsychotics in human serum by HPLC tandem mass spectrometry: a multi-level, single-sample approach, Journal of Chromatography B, 843 (2006) 100-113.

[16] H. Tokunaga, K. Kudo, N. Jitsufuchi, Y. Ohtsuka, T. Imamura, Sensitive determination of sulpiride in human plasma by high-performance liquid chromatography, Journal of Chromatography B: Biomedical Sciences and Applications, 691 (1997) 203-207.

[17] M.I. Walash, M.M.K.S. El-din, N.M. El-enany, M.I. Eid, S.M. Shalan, Simultaneous determination of sulpiride and mebeverine by HPLC method using fluorescence detection: application to real human plasma, Chemistry Central Journal, 6 (2012) 13.

[18] M. C. Huang, H. O. Ho, G. C. Yeh, W. T. Ke, L. C. Lin, T.-M.B. Hsu, C.-C. Kao, M.-T. Sheu, Development of a high-performance liquid chromatographic method for bioanalytical applications with sulpiride, Journal of Chromatography B: Biomedical Sciences and Applications, 763 (2001) 157-163.

[19] L. Shi-Iian, L. Chuan-hua, Q. Yan-Jiang, Z. Quan-qin, L. Xian-xi, L. Feng-li, Simultaneous Determination of Sulpiride, Clozapine and Chlorpromazine in Human Plasma by HPLC, Chinese Journal of Pharmaceutical Analysis, 5 (2002) 007.

[20] M.A. Mohamed, A.M. Yehia, C.E. Banks, N.K. Allam, Novel MWCNTs/graphene oxide/pyrogallol composite with enhanced sensitivity for biosensing applications, Biosensors and Bioelectronics, 89 (2017) 1034-1041.

[21] M.A. Mohamed, S.A. Atty, N.N. Salama, C.E. Banks, Highly Selective Sensing Platform Utilizing Graphene Oxide and Multiwalled Carbon Nanotubes for the Sensitive Determination of Tramadol in the Presence of Co-Formulated Drugs, Electroanalysis, 29 (2017) 1038-1048.

[22] S. Gheibi, H. Karimi-Maleh, M.A. Khalilzadeh, H. Bagheri, A new voltammetric sensor for electrocatalytic determination of vitamin C in fruit juices and fresh vegetable juice using modified multi-wall carbon nanotubes paste electrode, Journal of Food Science and Technology, 52 (2015) 276-284.

[23] H. Bagheri, N. Pajooheshpour, B. Jamali, S. Amidi, A. Hajian, H. Khoshsafar, A novel electrochemical platform for sensitive and simultaneous determination of dopamine, uric acid

and ascorbic acid based on Fe_3O_4 SnO_2 Gr ternary nanocomposite, Microchemical Journal, 131 (2017) 120-129.

[24] M.A. Mohamed, Wearable miniaturized electrochemical sensors: benefits and challenges, Electrochemistry: The Royal Society of Chemistry, 15 (2019) 147-185. what is the name of the journal?

[25] M. A. Mohamed, A.S. Saad, S.H. Koshek, M.R. El-Ghobashy, Smart electrochemical sensing platform for the simultaneous determination of psychotic disorder drugs isopropamide iodide and trifluoperazine hydrochloride, New Journal of Chemistry, 42 (2018) 9911-9919.

[26] M.A. Mohamed, F.M. El-badawy, H.S. El-Desoky, M.M. Ghoneim, Magnetic cobalt ferrite nanoparticles $CoFe_2O_4$ platform as an efficient sensor for trace determination of Cu(II) in water samples and different food products, New Journal of Chemistry, 41 (2017) 11138-11147.

[27] K.S. Novoselov, A.K. Geim, S.V. Morozov, D. Jiang, Y. Zhang, S.V. Dubonos, I.V. Grigorieva, A.A. Firsov, Electric field effect in atomically thin carbon films, Science, 306 (2004) 666-669.

[28] S. Szunerits, R. Boukherroub, Graphene-based nanomaterials in innovative electrochemistry, Current Opinion in Electrochemistry, 10 (2018) 24-30.

[29] L. Wang, A. Wu, G. Wei, Graphene-based aptasensors: from molecule–interface interactions to sensor design and biomedical diagnostics, Analyst, 143 (2018) 1526-1543.

[30] L. Wang, Y. Zhang, A. Wu, G. Wei, Designed graphene-peptide nanocomposites for biosensor applications: A review, Analytica Chimica Acta, 985 (2017) 24-40.

[31] S. Hu, Y. Wang, X. Wang, L. Xu, J. Xiang, W. Sun, Electrochemical detection of hydroquinone with a gold nanoparticle and graphene modified carbon ionic liquid electrode, Sensors and Actuators B: Chemical, 168 (2012) 27-33.

[32] M.A. Mohamed, S.A. Atty, H.A. Merey, T.A. Fattah, C.W. Foster, C.E. Banks, Titanium nanoparticles (TiO_2)/graphene oxide nanosheets (GO): an electrochemical sensing platform for the sensitive and simultaneous determination of benzocaine in the presence of antipyrine, Analyst, 142 (2017) 3674-3679.

[33] D. Li, M.B. Müller, S. Gilje, R.B. Kaner, G.G. Wallace, Processable aqueous dispersions of graphene nanosheets, Nature Nanotechnology, 3 (2008) 101.

[34] Y. Si, E.T. Samulski, Exfoliated graphene separated by platinum nanoparticles, Chemistry of Materials, 20 (2008) 6792-6797.

[35] J. Yan, Z. Fan, W. Sun, G. Ning, T. Wei, Q. Zhang, R. Zhang, L. Zhi, F. Wei, Advanced asymmetric supercapacitors based on Ni(OH)$_2$/graphene and porous graphene electrodes with high energy density, Advanced Functional Materials, 22 (2012) 2632-2641.

[36] H. Du, L. Jiao, K. Cao, Y. Wang, H. Yuan, Polyol-mediated synthesis of mesoporous α-Ni (OH) 2 with enhanced supercapacitance, ACS Applied Materials & Interfaces, 5 (2013) 6643-6648.

[37] Z. Lu, Z. Chang, W. Zhu, X. Sun, Beta-phased Ni(OH)$_2$ nanowall film with reversible capacitance higher than theoretical Faradic capacitance, Chemical Communications, 47 (2011) 9651-9653.

[38] P. Oliva, J. Leonardi, J. Laurent, C. Delmas, J. Braconnier, M. Figlarz, F. Fievet, A.d. Guibert, Review of the structure and the electrochemistry of nickel hydroxides and oxy-hydroxides, Journal of Power Sources, 8 (1982) 229-255.

[39] M. Aghazadeh, A.N. Golikand, M. Ghaemi, Synthesis, characterization, and electrochemical properties of ultrafine β-Ni(OH)$_2$ nanoparticles, International Journal of Hydrogen Energy, 36 (2011) 8674-8679.

[40] Y.H. Huang, J.H. Chen, X. Sun, Z.B. Su, H.T. Xing, S.R. Hu, W. Weng, H.X. Guo, W.B. Wu, Y. San He, One-pot hydrothermal synthesis carbon nanocages-reduced graphene oxide composites for simultaneous electrochemical detection of catechol and hydroquinone, Sensors and Actuators B: Chemical, 212 (2015) 165-173.

[41] N. Karikalan, M. Velmurugan, S.-M. Chen, C. Karuppiah, Modern approach to the synthesis of Ni (OH) 2 decorated sulfur doped carbon nanoparticles for the nonenzymatic glucose sensor, ACS Applied Materials & Interfaces, 8 (2016) 22545-22553.

[42] Y. Zhang, W. Lei, Q. Wu, X. Xia, Q. Hao, Amperometric nonenzymatic determination of glucose via a glassy carbon electrode modified with nickel hydroxide and N-doped reduced graphene oxide, Microchimica Acta, 184 (2017) 3103-3111.

[43] A.L. Sanati, H. Karimi-Maleh, A. Badiei, P. Biparva, A.A. Ensafi, A voltammetric sensor based on NiO/CNTs ionic liquid carbon paste electrode for determination of morphine in the presence of diclofenac, Materials Science and Engineering: C, 35 (2014) 379-385.

[44] T. Tavana, M.A. Khalilzadeh, H. Karimi-Maleh, A.A. Ensafi, H. Beitollahi, D. Zareyee, Sensitive voltammetric determination of epinephrine in the presence of acetaminophen at a novel

ionic liquid modified carbon nanotubes paste electrode, Journal of Molecular Liquids, 168 (2012) 69-74.

[45] W.S. Hummers Jr, R.E. Offeman, Preparation of graphitic oxide, Journal of the American Chemical Society, 80 (1958) 1339-1339.

[46] M.A. Mohammed, A.K. Attia, H.M. Elwy, Electrochemical Sensor Based on Multiwalled Carbon Nanotube, Alizarine Red S and Chitosan for Simultaneous Determination of Oxomemazine Hydrochloride, Paracetamol and Guaifenesin, Electroanalysis, 29 (2017) 506-513.

[47] R.G. Compton, C.E. Banks, Understanding voltammetry, World Scientific, 2007.

[48] S. Bykkam, K. Rao, C. Chakra, T. Thunugunta, Synthesis and characterization of graphene oxide and its antimicrobial activity against klebseilla and staphylococus, International Journal of Advanced Biotechnology and Research, 4 (2013) 142.

[49] D.-L. Fang, Z.-D. Chen, X. Liu, Z.-F. Wu, C.-H. Zheng, Homogeneous growth of nano-sized β-Ni(OH)$_2$ on reduced graphene oxide for high-performance supercapacitors, Electrochimica Acta, 81 (2012) 321-329.

[50] S. Min, C. Zhao, G. Chen, X. Qian, One-pot hydrothermal synthesis of reduced graphene oxide/Ni (OH) 2 films on nickel foam for high performance supercapacitors, Electrochimica Acta, 115 (2014) 155-164.

[51] X.a. Chen, X. Chen, F. Zhang, Z. Yang, S. Huang, One-pot hydrothermal synthesis of reduced graphene oxide/carbon nanotube/α-Ni (OH) 2 composites for high performance electrochemical supercapacitor, Journal of Power Sources, 243 (2013) 555-561.

[52] L. Xu, Y.-S. Ding, C.-H. Chen, L. Zhao, C. Rimkus, R. Joesten, S.L. Suib, 3D Flowerlike α-Nickel Hydroxide with Enhanced Electrochemical Activity Synthesized by Microwave-Assisted Hydrothermal Method, Chemistry of Materials, 20 (2008) 308-316.

[53] J.W. Lee, T. Ahn, D. Soundararajan, J.M. Ko, J.-D. Kim, Non-aqueous approach to the preparation of reduced graphene oxide/α-Ni (OH)$_2$ hybrid composites and their high capacitance behavior, Chemical Communications, 47 (2011) 6305-6307.

[54] L. Xu, Y.-S. Ding, C.-H. Chen, L. Zhao, C. Rimkus, R. Joesten, S.L. Suib, 3D flowerlike α-nickel hydroxide with enhanced electrochemical activity synthesized by microwave-assisted hydrothermal method, Chemistry of Materials, 20 (2007) 308-316.

[55] B. Li, H. Cao, J. Shao, H. Zheng, Y. Lu, J. Yin, M. Qu, Improved performances of β-Ni $(OH)_2$@ reduced-graphene-oxide in Ni-MH and Li-ion batteries, Chemical Communications, 47 (2011) 3159-3161.

[56] E. Laviron, L. Roullier, C. Degrand, A multilayer model for the study of space distributed redox modified electrodes: Part II. Theory and application of linear potential sweep voltammetry for a simple reaction, Journal of Electroanalytical Chemistry and Interfacial Electrochemistry, 112 (1980) 11-23.

[57] A.J. Bard, L.R. Faulkner, J. Leddy, C.G. Zoski, Electrochemical methods: fundamentals and applications, wiley New York, 1980.

[58] I.C.H. Guidelines, Q2B validation of analytical procedures: methodology, Fed. Regist, 62 (1997).

TOC

0.4 M NaOH,
Hydrothermal conditions at
160 °C for 14 h

Graphene Oxide (GO)

Ni^{+2}

$\beta\text{-}Ni(OH)_2.Gr$